

DOI: <https://doi.org/10.37434/tpwj2024.05.04>

OPTIMIZATION OF THE METAL POOL SHAPE DURING ELECTROSLAG SURFACING IN A STATIONARY CURRENT-SUPPLYING MOULD FOR MANUFACTURE OF BIMETALLIC PRODUCTS

V.G. Solovyov, Yu.M. Kuskov, I.Yu. Romanova

E.O. Paton Electric Welding Institute of the NASU
11 Kazymyr Malevych Str., 03150, Kyiv, Ukraine

ABSTRACT

Mathematical modeling of multiphysics processes of Joule heating has been conducted using a finite element model of a stationary current-supplying mould (CSM). To manufacture bimetallic products using a stationary current-supplying mould with a circular cross-section during melting of a discrete additive at its batch feeding, the study presents the results of calculated assessment of the dependence of such metal pool shape parameters as the mirror diameter and the liquid fraction depth on the slag pool depth and CSM design parameters, namely the mould diameter, the thickness of copper bushings in the mould current-supplying and forming sections, the water-cooled bottom plate thickness, and the variations in the graphite lining height caused by wear. The findings will contribute to improvement of the mould design, optimization of the metal pool shape, and the technology of discrete additive melting at batch feeding in a stationary CSM.

KEYWORDS: stationary current-supplying mould, metal pool parameters, shape optimization, multiphysics modeling, electroslag surfacing, bimetallic product

INTRODUCTION

The method of surfacing and remelting in a current-supplying mould (CSM) [1] has specific features determined by the design of this device. First of all, it represents a section nonconsumable electrode of a circular type. In CSM, the lower section, electrically isolated from the upper one, is the forming one (FMS), in which the metal pool (MP) is formed. The second nonconsumable electrode represents a bottom plate or a product being formed. In addition, due to a vertical cut in a current-supplying section, a magnetic field is generated in the melt, due to which, the rotation of slag (SP) and metal pools in the horizontal plane is provided. Stationary CSM has one more important feature – comparatively small ingots (not more than 60 mm) are deposited in it.

Ksendzyk G.V., the author of the idea and the base model of a current-supplying mould, suggested to use a “clamping device for current supply connected to the device for additive feeding to the slag pool” as a means to influence the crystallization front shape of the molten metal in the FMS. This enabled an adjustment of the MP shape by means of varying the current direction and value in the clamping device. This allows making it more flat and thus reducing the risk of defects in crystals [2, 3].

This is especially important for fusion of bimetallic parts. Flat MP is achieved by selecting the optimal ratio of currents, voltages and feed rate of a consumable electrode or a consumable discrete additive, as well as the thermal level of the SP and the intensity of heat sink

through the mould walls [4]. The geometric CSM parameters, such as the diameters of the mould and electrode (consumable and nonconsumable), the distance between the MP mirror and the lower end of the graphite lining (GL), the thickness of the electric insulating gasket between the both sections of the mould and bottom plate, have a great effect on the MP formation. A series of works has been devoted to the control of the metal pool formation process [5, 6]. In [5], a conclusion is made, that a flat MP shape can be obtained in a double-circuit surfacing at appropriate power ratios on the mould and electrode. In [6], different existing methods and technological techniques of the metal crystallization control in electroslag remelting are characterized, which are based on the use of metallurgical mechanisms and external physical influences. It has been concluded that the control of the process of primary crystallization of ingots, especially complex alloys and ingots of large diameters, remains one of the key tasks in the further development of electroslag technologies. In [7], the method of impact on the metal pool shape by means of the external magnetic field is used. Thus, the traditional Joule heating and stirring of the liquid metal under the influence of a directed magnetic field are combined.

As indices of the MP shape, geometric data of its sizes such as the relative average for the product surface, penetration depth and relative penetration unevenness [8, 9], as well as height of the cylindrical part of MP are used. In the best case, the optimal MP shape should be minimal in height and have a cylindrical shape.

In [10], the authors came to the conclusion that the average mould section, which is conducting, shunts a

part of SP and shifts the area of a predominant heat sink into the near-wall area, leaving the central zone relatively cold. However, directly near the mould wall itself, the MP remains relatively cold due to water cooling of the mould. As a result, the MP bottom can take a specific shape of “sombbrero”. The shape of the MP bottom in the form of “sombbrero” is characterized by a large relative unevenness of the MP, so it requires optimization.

Mathematical modeling of heat exchange, melting and solidification processes in the electroslag technology becomes an effective means of theoretical research [11–14].

THE AIM

of the work is to analyze the factors affecting the MP shape when manufacturing bimetallic products using a stationary CSM with a circular cross-section in the process of melting a discrete additive at its batch feeding, as well as to optimize the thermal physical processes of surfacing by means of mathematical modeling. Within the frames of a calculation experiment, the possibilities of improving the MP shape by variations in the CSM design were considered.

METHODS OF EXPERIMENTAL RESEARCH

In the work, the results of the experimental electroslag surfacing (ESS) of layers with a different thickness using a stationary current-supplying mould with a vertical cut in a current-supplying section were used [15]. This surfacing was conducted to study the nature of variation in the electrotechnical parameters of the discrete additive melting process at batch feeding. During the experiment, rotation of the SP was observed. AC voltage from the TShP-10 transformer with a sinusoidal voltage having four voltage variation degrees was supplied to the terminals of the current-supplying mould section (CSMS) and the mould bottom plate. The “liquid” start was used. A batch four-time shot feeding by 2 kg was performed. During the experiment, the voltage applied to the terminals of the copper CSMS bushing and the

bottom plate, as well as the current in the CSMS-slag pool-metal pool-product-bottom plate circuit were measured in time. The digital conversion of the mentioned parameters and the calculation of the conductivity and consumed power of the measured electrical circuit were performed. In the future, to simplify the presentation, the obtained electrical parameters were attributed to the CSM as a whole. Figure 1 shows the nature of variation in the CSM electrical conductivity in the process of the experiment.

After switching the current source from the 4th to the 3rd degree, the voltage in the CSM changed from 51 to 43 V. The shot charging was accompanied by a gradual increase in the CSM current and electrical conductivity even after the end of charging. This was partially explained by a decrease in the slag layer level between the molten metal layer on the bottom plate and the graphite lining of the CSMS, as well as an increase in the SP temperature due to a rise in the current (from 1.9 to 2.8 kA). A drop in the current was achieved by switching to the 2nd and then to the 1st degree of the power source. In the physical experiment, CSM with the following design parameters was used: internal mould diameter $D_m = 180$ mm; CSMS height $h_{CSMS} = 90$ mm; FMS height $h_{FMS} = 73$ mm; GL height $h_{gl} = 65$ mm; GL thickness $T_{gl} = 15$ mm; SP depth $h_{sp} = 70$ mm.

Stages of surfacing (Figure 1): t_1 — liquid slag pouring, switching on the power source to the 4th degree; t_2 — increase in the slag rotation; t_3 — 3rd degree is switched on; t_4 — the process runs stable; t_5 — beginning of feeding the 1st shot batch; t_6 — end of feeding the 1st shot batch; t_7 — beginning of feeding the 2nd shot batch; t_8 — end of feeding the 2nd shot batch; t_9 — beginning of feeding the 3rd shot batch; t_{10} — end of feeding the 3rd shot batch; t_{11} — beginning of feeding the 4th shot batch; t_{12} — end of feeding the 4th shot batch; t_{13} — the 2nd degree is switched on; t_{14} — the 1st degree is switched on; t_{15} — pool rotation is normal; t_{16} — switching off the power source.

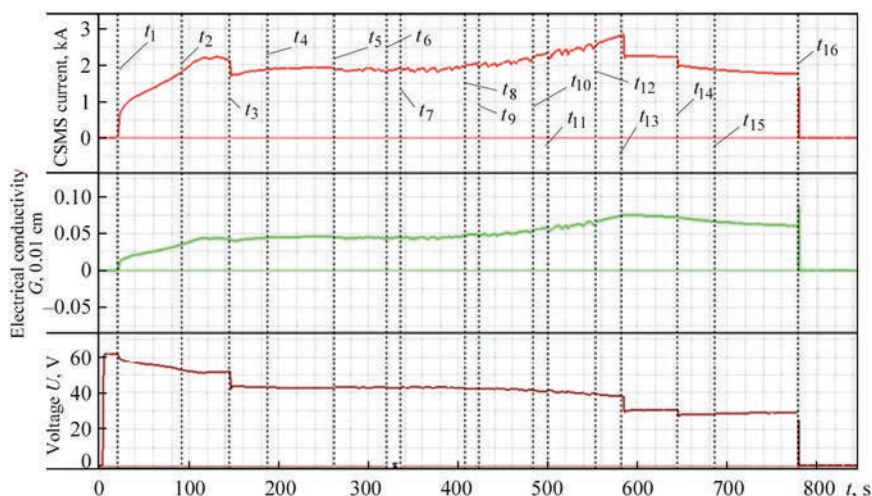


Figure 1. Variation in current, electrical conductivity and voltage on CSM over time in the process of surfacing

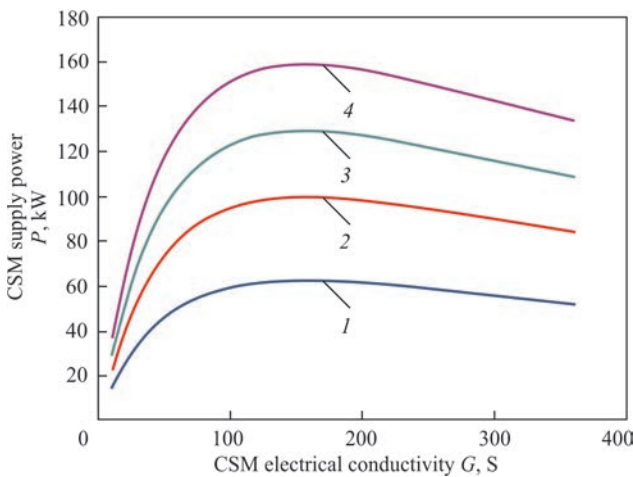


Figure 2. Dependences of power, consumed by the mould, on the CSM electrical conductivity for four degrees of voltage variation of the TShP-10 power source, obtained during surfacing: 1 — first degree; 2 — second degree; 3 — third degree; 4 — fourth degree

In the experiment, ANF-29 flux (melting point is 1230–1250 °C); the shot being deposited from chromium cast iron, batch by 2 kg were used. During melting, a shot batch turned into a liquid metal, which was subsequently solidified in the form of a deposited layer of ~12 mm thick.

Based on the results of the experiment data analysis, the dependence of the specific electrical conductivity of ANF-29 flux σ_{sp} on the SP temperature at a hypothetical point of its maximum value $\sigma_{sp}[T_{max}] = 1.349 \cdot 10^{-3} T_{max}^{1.638} + 138.2$ was obtained for the temperature range of 1000–2000 °C. A hypothetical point of the maximum value of the SP temperature is a point, at which the SP temperature reaches the highest value at set electroslag process parameters. The maximum value of the SP temperature at a hypothetical point was determined as a result of calculating the thermal SP field using an additional CSM substitution design model, similar to that described in [15].

Based on the results of the analysis, the dependencies of power consumed by the CSM on the CSM

electrical conductivity for four degrees of the power source were obtained (Figure 2).

The data of these dependencies were used to predict surfacing parameters that were not obtained during a physical experiment. Analytical appearance of the obtained dependences is the following:

$$P(G) = a \exp(bG) + c \exp(dG)$$

where for the 1st degree: $a = 77.16$; $b = -0.001076$; $c = -75.78$; $d = -0.02025$; for the 2nd degree: $a = 124.0$; $b = -0.0011076$; $c = -121.8$; $d = -0.02025$; for the 3rd degree: $a = 160.6$; $b = -0.001076$; $c = -157.7$; $d = -0.02025$; for the 4th degree: $a = 197.6$; $b = -0.001076$; $c = -194.0$; $d = -0.02025$. Determination coefficient is $R = 0.9999$.

The data obtained as a result of the experiment were used to create and validate the ESS mathematical model of in the CSM.

MULTIPHYSICS MODELING

Multiphysics modeling was performed on a graphic three-dimensional model (Figure 3, *a*) with modeling of the Joule heating. The model contains the upper current-supplying mould section, consisting of a copper water-cooled bushing without a vertical cut and a graphite lining, as well as the lower forming mould section, which is the second copper bushing. In addition, the model contains a slag pool, a product, a bottom plate, a skull between the forming section and the SP/product, as well as asbestos insulation between the sections of the mould and bottom plate.

By means of the magnetic field generated by the current-supplying mould section, the rotation of slag and metal pools in the horizontal plane is provided. As a result, heating of the external water-cooled SP edges and heat sink from its maximum heating zones is intensified, which in itself leads to the thermal SP field equalization in a horizontal cross-section and an increase in the intensification of the surfacing process and the consumed power. However, in the scien-

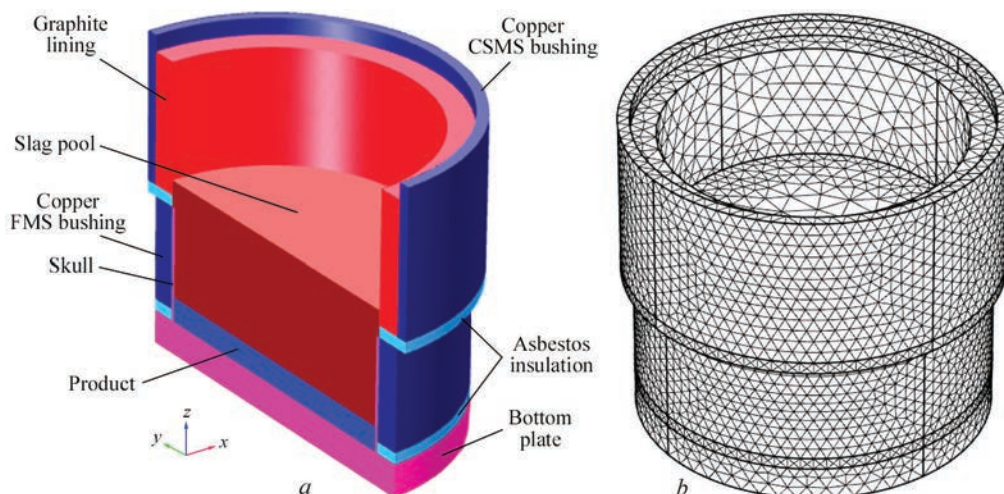


Figure 3. Examples of model scheme: *a* — CSM design; *b* — finite element model of CSM

Table 1. Physical properties of materials for modeling

Parameter	Product	Slag	Graphite	Asbestos	Copper
Heat conductivity C_p , J/(kg·K)	475	1200	710	1000	385
Relative dielectric permeability ε	1	1	1	5	1
Density ρ , kg/m ³	7850	8960	1950	$\rho[T]$	8940
Thermal conductivity k , W/(m·K)	44.5	60	150	$k[T]$	400
Temperature expansion coefficient α , 1/K	$12.3 \cdot 10^{-6}$	–	–	–	$3.862 \cdot 10^{-3}$
Specific electrical conductivity σ , S/m	$4.032 \cdot 10^6$	$\sigma_{sp}[T]$	$2 \cdot 10^5$	$4.032 \cdot 10^{-6}$	$5.998 \cdot 10^7$

tific literature, there are different opinions about the electromagnetic effect on the depth of a metal pool, formed during the electroslag process. As noted by Ksendzyk G.V. in [16], “some of them believe that simple rotation of slag and metal pools leads to an increase in the MP depth and only a reciprocating movement ensures its decrease”. We believe that the solution of a hydrodynamic problem associated with the movement of liquid in the slag pool can adjust certain values of the metal pool depth relative to that calculated using the presented model. We also believe that the trends of the effect of variations in the geometric parameters of the model on the MP shape will not change. In connection with the stated above, when modeling a current-supplying mould, we did not use an split current-supplying section, which provides the rotation of slag and metal pools in the horizontal plane, did not solve the hydrodynamic problem, but limited to electromagnetic and thermal models.

Based on the provisions of the theory of similarity [17], a geometric model was created, that takes into account the similarity of its geometric parameters with the geometric parameters of the physical model. The main condition for modeling was to provide the maximum correspondence of the geometric part of the model with the geometric parameters and the results of the physical experiment. The physical properties of the materials of the slag, welding product and electrodes were used (Table 1).

The model uses the following design parameters: internal mould diameter $D_m = 180$ mm; CSMS height $h_{CSMS} = 90$ mm; FMS height $h_{FMS} = 74$ mm; GL height $h_{gl} = 80$ mm; GL thickness $T_{gl} = 15$ mm; SP depth $h_{sp} = 90$ mm; thickness of copper CSMS bushing, the surface of which is cooled with water $l_{gl} = 7$ mm; thickness of copper FMS bushing, the surface of which is cooled with water $h_{cb} = 15$ mm; asbestos insulation gasket height $h_i = 7$ mm; product height $h_{ph} = 15$ mm; bottom plate height $h_{b,p} = 20$ mm.

Parameters $\rho[T]$, $k[T]$ are set by the appropriate approximation dependencies on the temperature T , K (not given in the article).

The SP is heated at the expense of the Joule heat released while passing the electric current through it. To study the distribution of electric field, current and

potential in slag and metal pools, as well as to analyze the heat distribution in the volume of the studied zone, a finite element model was used (Figure 3, b).

The model solves the following thermal conductivity equations:

$$\rho(T)C_p \frac{\partial T}{\partial t} + \nabla \cdot q = Q,$$

where $q = -k(T)\nabla T$; Q is the additional heat source (in capacity of which, a heated metal pool can be used), W/m³; q is the heat flow density, W/m².

In the stationary coordinate system, the point form of the Ohm's law has the following appearance: $J = \sigma(T)E$; where J is the current density, A/m²; E is the electric field strength, V/m. The static form of the equation of current continuity in the electrically conductive environment requires: $\nabla J = -\nabla\sigma(T)\nabla U = 0$, where U is the voltage on CSM, V.

In the model, a stationary problem is solved and the results of the already established process are derived. The model allows determining the potential, current density and temperature at each point of the studied space in different variations (within the parameters determined by the technology) of the mould diameter, product thickness, distance between the MP and the lower CSMS edge, SP depth, etc.

The following restrictions were accepted for calculating the parameters of multiphysics processes in the model:

- hydrodynamic processes in the slag pool are not considered;
- device for water cooling of copper CSMS and FMS bushings and bottom plate is not considered;
- electrical contacts of the model are free side surfaces of the CSMS electrode and bottom plate;
- supplied voltage on the CSM does not exceed 15–60 V;
- power source current does not exceed 7 kA;
- the maximum value of the temperature T_{max} of heating SP elements does not exceed the boiling point of the slag. In the model, $T_{max} = 1800$ °C;
- thermal losses due to radiation are not considered;
- the values of only set parameters after the transition process are considered.

Based on the results of analysing the data obtained from the experiment, the dependence of the specific electrical conductivity of ANF-29 flux on the SP temperature at the point of its maximum value is determined. This dependence was used to control T_{\max} when calculating modeling results with the aim not to exceed it. If as a result of the mathematical experiment at set input parameters, T_{\max} exceeds the boiling point of the slag, then the values of input parameters are reviewed.

MATHEMATICAL EXPERIMENTS ON THE MP FORMATION

INFLUENCE OF THE SLAG POOL DEPTH ON THE METAL POOL SHAPE

The impact of a growth in the SP depth on its thermal level at a constant interelectrode distance was considered under the following initial conditions: distance between the product and the level of the lower CSMS edge $H_{pgl} = 73$ mm; SP depth $h_{sp} = 90$ mm; voltage on the CSM relative to the bottom plate $U = 42.7$ V. The calculation under these initial conditions showed that the maximum SP temperature at the level of the lower CSMS edge $T_{CSMS} = 1767$ °C; the maximum MP mirror temperature $T_{MP} = 1450$ °C; the electrical conductivity of the mould $G_m = 44.5$ S; the consumption power $P_m = 81.1$ kW; the maximum depth of the liquid part of MP $H_{if} = 6.7$ mm; the depth of the interfacial part of MP $H_{mp} = 2$ mm.

After an increase in the SP depth by 40 mm (from 90 to 130 mm), the values of other parameters being constant, the calculation showed the following: the maximum SP temperature at the level of the lower CSMS edge $T_{CSMS} = 1627$ °C; the maximum MP mirror temperature $T_{MP} = 1525$ °C; the electrical conductivity of the mould $G_m = 49.9$ S; the consumption power $P_m = 91$ kW; the maximum depth of the liquid part of MP $H_{if} = 9.6$ mm; the depth of the interfacial part of MP $H_{mp} = 2$ mm.

The relative impact of the SP depth, other geometric parameters being constant, on the power consumed by the process, the CSM electrical conductivity and the MP depth is the following: $\delta P_m = (91 - 81.1)/40 = 0.25$; $\delta G_m = (49.9 - 44.5)/40 = 0.135$; $\delta h_{mp} = (9.6 - 6.7)/40 = 0.0725$.

From this it follows that an increase in the SP depth, other geometric parameters being constant,

leads to an increase in the MP depth. For example, an increase in the SP depth by 10 mm leads to an increase in the MP depth by ~ 0.7 mm.

IMPACT OF THE WEAR VALUE OF THE LOWER EDGE OF THE GRAPHITE LINING ON THE METAL POOL SHAPE

The impact of the wear O_{gl} of the lower edge of the graphite lining of the CSMS as a result of operation on the power consumed by the mould, electrical conductivity and MP depth is considered. For the calculations, six values of the GL wear height relative to its initial location were accepted, bearing in mind that at the value $O_{gl} = 0$, the calculation was carried out in the p. 1. The results are given in Table 2.

In Nos 5 and 6 of the experiment, the lack of the pool is predetermined by the absence of the required level of power released in the slag pool under these created conditions.

The data (Table 2) indicate a significant impact of the wear of the lower GL edge on the MP formation. This phenomenon is associated with sharp cooling of the SP, caused by a direct contact of the slag with a water-cooled copper bushing. It is important to keep in mind that depletion of the wall in the copper CSMS bushing can lead to its rapid wear due to electric erosion, especially taking into account, that the lower CSMS edge is characterized by the highest current density, flowing in the mould. In addition, an increase in the GL production leads to an increase in the contact area with the slag and, accordingly, to an increase in the temperature of the copper bushing wall that borders it. The larger the area of the current-conducting bushing is protected by graphite, the lower probability of damages to the bushing in this place with erosion and the greater the probability that with some small area of an unprotected bushing and the corresponding low current density passing through this part, the formation of slag crust on this small surface area is probable. Therefore, at some point and within some time, there may be a replacement of graphite protection of some part of the copper surface with the help of a slag crust. But since the current-supplying section is connected to the power source, with the further increase in the area of unprotected graphite of the copper bushing, the copper wall will be heated to the melting point (about 1100 °C) and an emergency situation may occur.

Table 2. Impact of wear of the lower GL edge on the metal pool shape

Exp. No.	GL wear O_{gl} , mm	Power P_m , kW	CSM conductivity G_m , S	MP depth H_{if} , mm	MP mirror diameter O_{mp} , mm
1	0.1	80.2	44.0	6.7	176
2	1	79.6	43.6	6.2	176
3	4	77.2	42.3	4.28	146
4	8	73.9	40.6	1	74
5	12	70.7	38.7	–	No pool
6	16	67	36.8	–	

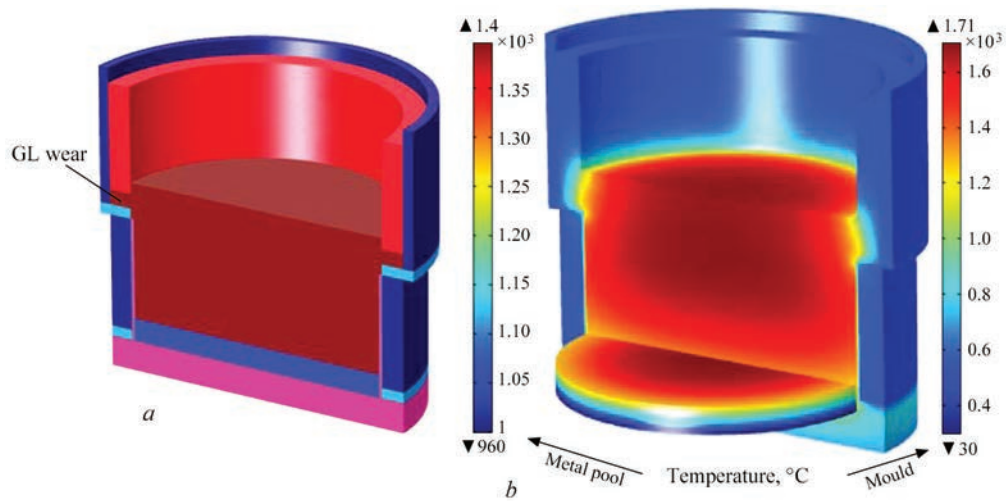


Figure 4. Examples of modeling results: *a* — graphite lining wear location; *b* — graphic temperature distribution in CSM at GL deformation

Figure 4 shows fragments of GL wear modeling.

IMPACT OF VARIATION IN THE THICKNESS OF THE COPPER CSMS BUSHING ON THE METAL POOL SHAPE

The thickness of the water-cooled upper CSMS and the lower FMS copper bushings, as well as the thickness of the water-cooled bottom plate together with the workpiece determine the consumed component of the CSM thermal balance. As a result of variation in the thicknesses of the mentioned components of the CSM design at a constant voltage, it is possible to change the thermal level of the surfacing process and influence the MP shape.

The created model was used to analyze the level of the impact of the variation in the wall thickness of the copper CSMS bushing l_{sw} on P_m , G_m and H_{if} . The initial value $l_{sw} = 7$ mm. Table 3 shows the results of calculations of the impact of the thickness of the copper CSMS bushing on the MP parameters. The calculations were performed at the voltage on the CSM $U = 35.7$ V, the distance between the MP mirror and the lower CSMS edge is 58 mm.

The given data indicate that at a voltage being constant, there is almost no impact of the wall thickness of the copper CSMS bushing on the electrical conductivity of the mould, consumed power and the temperature of the bushing side bordering on the GL. The variation in the wall thickness has a relatively small impact on the MP depth. As the wall thickness of the copper CSMS bushing becomes larger, the MP depth increases slightly and the mirror diameter or the

height of the cylindrical part of the MP grows slightly. This is explained by the fact that with an increase in the wall thickness of the copper CSMS bushing, the thermal level of the SP grows due to reduction in losses through the bushing. At a constant value of the power consumption, the MP heating grows. This is accompanied by an increase in the depth and width of the MP. The fact that a slight variation in the wall thickness leads to the variation in the temperature of the bushing side, which borders on the GL, indicates that the wall thickness can still be reduced to a certain value, which depends on the arrangement of the system for cooling the copper bushing. At the same time, the MP depth will decrease.

Due to the fact, that the CSMS bushing is under the thermal and electric protection of the GL, it becomes necessary to check the possibility of replacing the copper bushing with a steel one, which is less expensive.

REPLACING THE COPPER CSMS BUSHING WITH A STEEL ONE

Impact on the metal pool shape. The experiment was conducted in the conditions similar to those specified in the p. 3 of the section. For the experiment, St3 steel was selected. The presented data (Table 4) confirm that when replacing the copper CSMS bushing with a steel one and while keeping the same voltage on the CSM, as in the previous experiment, the consumed CSM power and electrical conductivity remained unchanged. However, an increase in the thermal impact on the MP was observed, which led to an increase in its depth and the mirror diameter. Hence, it follows

Table 3. Analysis of the impact of the wall thickness of the copper CSMS bushing on the MP parameters

Exp. No.	Thickness of copper wall l_{gp} , mm	Power P_m , kW	CSM conductivity G_m , S	MP depth H_{if} , mm	MP mirror diameter \varnothing_{mp} , mm	Temperature of the copper wall, °C
1	7	71.9	56.5	7.2	162	571
2	11	72.0	56.5	7.4	162	580
3	15	72.0	56.5	7.5	164	590

Table 4. Analysis of the impact of replacing the copper CSMS bushing with a steel one on the metal pool shape

Exp. No.	Thickness of steel wall l_{sw} , mm	Power P_m , kW	CSM conductivity G_m , S	MP depth H_{if} , mm	MP mirror diameter \varnothing_{mp} , mm	Temperature of the steel wall, °C
1	7	71.9	56.5	8.8	172	701
2	11	72.0	56.5	9.7	176	761
3	15	72.0	56.5	10.4	176	810

Table 5. Analysis of the impact of the wall thickness of the copper FMS bushing on the MP parameters

Exp. No.	Thickness of copper wall h_{cb} , mm	Power P_m , kW	CSM conductivity G_m , S	MP depth H_{if} , mm	MP mirror diameter \varnothing_{mp} , mm	Temperature of the copper wall, °C
1	7	76.1	56.5	7	167	559
2	11	76.2	56.5	7.2	167.8	565
3	15	76.2	56.6	10.2	170.2	588

that by reducing the voltage on the CSM and, accordingly, reducing the consumed power of the CSM, it is possible to return the characteristics of the MP to the values similar to the previous experiment (p. 3).

IMPACT OF VARIATION IN THE THICKNESS OF THE COPPER FMS BUSHING ON THE METAL POOL SHAPE

The experiment was carried out in the conditions similar to p. 3. Table 5 shows the calculation data of the impact of the thickness of the water-cooled copper bushing of the forming FMS section h_{cb} on P_m , G_m and H_{if} .

The mentioned data indicate that at a constant voltage, the impact of the wall thickness of the copper FMS bushing on the electrical conductivity of the mould and its consumed power is almost absent. The variation in the wall thickness has a significant effect on the MP depth than the variation in the thickness of the copper CSMS wall due to the presence of a thermal insulating GL in the CSMS. As the wall thickness of the copper FMS bushing becomes larger, the MP depth grows, and the diameter of the MP mirror increases. This is explained by the fact that with an increase in the wall thickness of the copper FMS bushing, the thermal level of the SP grows due to reduction in the heat losses through the bushing. At a constant value of the consumed power, the MP heating grows, which is accompanied by an increase in the depth and

width of the MP. This is important when it is necessary to increase the diameter of the MP mirror to the maximum value at a set voltage.

IMPACT OF VARIATION IN THE THICKNESS OF THE WATER-COOLED BOTTOM PLATE ON THE METAL POOL SHAPE

The experiment was carried out in the conditions similar to those described in p. 3. Table 6 shows the calculation data on the impact of the variation in the thickness of the water-cooled bottom plate $h_{b,p}$ on P_m , G_m and H_{if} . The product height in the experiment remains constant $h_{ph} = 30$ mm. The given data indicate that at a constant voltage of the power source, the impact of the variation in the bottom plate thickness on the electrical conductivity of the mould and its consumed power is almost absent.

The variation in the bottom plate thickness leads to an increase in the depth and diameter of the MP mirror. When reducing the bottom plate thickness and increasing the voltage on the CSM, the MP shape can be significantly improved. Figure 5 shows an example of the MP with a depth $H_{if} = 2.6$ mm and the mirror diameter of 176 mm at $U = 51$ V, bottom plate thickness of $h_{b,p} = 5$ mm, $P_m = 116$ kW and $G_m = 44.5$ S. In this example, as the bottom plate thickness is reduced, a limit on the maximum temperature value of the SP $T_{max} < 1800$ °C was reached.

When searching for the CSM and voltage configuration on the CSM to reach the minimum depth and the maximum diameter of the pool mirror, the conditions were kept, that the SP temperature in its maximum zone did not exceed 1800 °C and the voltage on the CSM did not exceed 60 V.

IMPACT OF THE VARIATION IN THE MOULD DIAMETER ON THE MP SHAPE

The experiment was carried out in the range of the variation in the mould diameter $D_m = 180-300$ mm. To obtain the sought parameters that will not exceed the operating ones, the voltage value on the CSM was taken as $U = 35$ V and the distance between the product

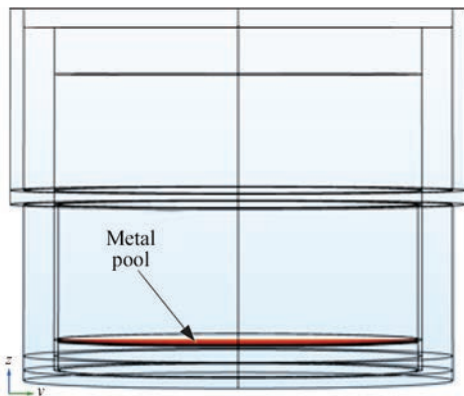


Figure 5. Example of metal pool with the minimum depth for the given CSM configuration with the minimum bottom plate thickness

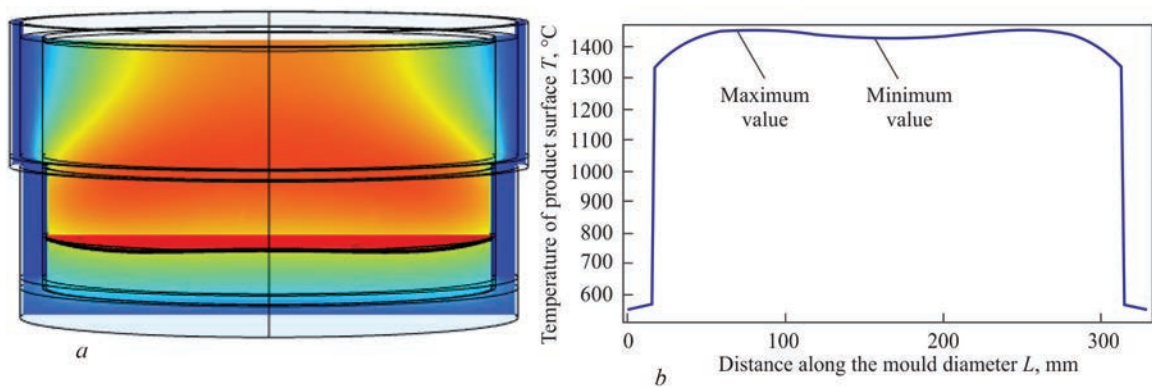
Table 6. Analysis of the impact of the bottom plate thickness on the MP parameters

Exp. No.	Thickness of bottom plate $h_{b,p}$, mm	Power P_m , kW	CSM conductivity G_m , S	MP depth H_{if} , mm	MP mirror diameter \varnothing_{mp} , mm	Max. temperature of the upper surface of the product, °C
1	20	71.9	56.5	7.2	162.0	1425
2	26	71.9	56.4	10.5	173.8	1464
3	30	71.9	56.4	12.5	176.0	1486

Table 7. Analysis of the impact of variation in the mould diameter on the MP parameters

Exp. No.	Mould diameter D_m , mm	Power P_m , kW	CSM conductivity G_m , S	MP depth H_{if} , mm	MP mirror diameter \varnothing_{mp} , mm	Max. temperature of the upper product surface, °C
1	180	74.4	60.8	10.6	176	1471
2	220	100.0	81.8	9.7	216	1451
3	260	126.0	102.8	5.7/7.5*	256	1402/1435*
4	300	152.0	124.0	5.1/7.1*	296	1355/1418*

*At the mould diameter of 260 mm and higher; the voltage on the CSM $U = 35$ V and the distance between the product and the level of the lower CSMS edge $H_{pgl} = 53$ mm, MP takes the form of “sombbrero” [9] (see Figure 6), which is characterized by two values of H_{if} parameters and the maximum values of the product surface temperature.

**Figure 6.** MP shape and temperature along the diameter of the upper product edge at the mould diameter of 260 mm: *a* — MP “sombbrero” shape; *b* — temperature distribution with the confirmation of unevenness in the form of “sombbrero” with the designation of the minimum and maximum temperature values

and the level of the lower edge of the CSMS was taken as $H_{pgl} = 53$ mm. The results are given in Table 7.

The presented data indicate that the voltage values on the CSM being stable and the distance between the product and the lower edge of the CSMS being constant, the MP mirror diameter grows almost proportional to the mould diameter. The power consumed by the mould and electrical conductivity grow by about 20 % faster. The maximum temperature of the upper product surface remains almost unchanged. At the same time, the MP depth decreases almost twice, which leads to an increase in the ratio of the mirror diameter to the depth (\varnothing_{mp}/H_{if}) from 16.6 to 58.

CONCLUSIONS

Based on the results of the analysis of the obtained experimental data, the dependence of the specific electrical conductivity of ANF-29 flux on the SP temperature at the point of its maximum value was constructed. The de-

pendences of the power consumed by the mould on the SP electrical conductivity for four degrees of operation of the TShP-10 power source were obtained.

Multiphysics modeling was performed, that allows modeling the Joule heating processes for manufacturing bimetallic products using a stationary current-supplying mould with a circular section in the process of melting a discrete additive at its batch feeding. The carried out mathematical experiments allowed finding the ways to optimize some values of the initial parameters of the surfacing process, including geometric CSM parameters.

The results obtained during the mathematical experiment showed that an increase in the SP depth, other geometric parameters being constant, leads to an increase in the MP depth. A significant impact of the wear of the lower GL edge on the MP parameters was revealed. As the wear increases, the depth and diameter of the MP decrease, the electrical conductivity and consumed power of the SP drop.

Replacing the copper CSMS bushing with a steel one while keeping voltage on the CSM has almost no impact on the variation in the power consumption and electrical conductivity, but leads to an increase in the MP depth and diameter.

The voltage on the CSM being constant, the impact of the variation in the wall thickness of the copper CSMS and FMS bushing on the electrical conductivity of the mould and its consumed power is almost absent.

The voltage on the CSM being constant, the impact of the variation in the bottom plate thickness on the electrical conductivity of the mould and its power is almost absent. However, an increase in the bottom plate thickness leads to an increase in the depth and diameter of the MP mirror.

As the mould diameter grows from 180 to 300 mm, the diameter of the MP mirror increases almost proportionally to the mould diameter. The power consumed by the mould and electrical conductivity rise by about 20 % faster. The maximum temperature of the upper product surface remains almost unchanged. At the same time, the MP depth is almost twice decreased, which leads to an increase in the ratio of the mirror diameter to the depth ($\frac{D_{mp}}{H_{if}}$) from 16.6 to 58.

Analysis of the research results will contribute in improvement of the mould design and the technology of the process of melting discrete additive at batch feeding in CSM.

REFERENCES

1. Ksendzyk, G.V., Frumin, I.I., Shirin, V.S. (1980) *Electroslag remelting and surfacing apparatus*. Pat. GB 1568746A. <https://patentimages.storage.googleapis.com/6c/fe/4a/9f-5b70c9345524/GB1568746A.pdf>
2. (1986) *Metallurgy of electroslag process*. Ed. by B.I. Medovar et al. Kyiv, Naukova Dumka [in Russian].
3. Kuskov, Yu.M., Grishchenko, T.I. (2019) Formation of metal pool in current-supplying mould at electroslag process. *The Paton Welding J.*, **4**, 33–36. DOI: <https://doi.org/10.15407/tpwj2019.04.07>
4. Mamyshev, V.A., Shinskii, O.I., Sokolovskaya, L.A. (2018) Intensification of internal and external heat sink at the manufacture of cast billets in molds with different properties. Report 2. *Metall i Lityo Ukrainy*, 300–301(5–6), 38–45 [in Russian].
5. Medovar, L.B., Tsykulenko, A.K., Chernets, A.V. et al. (2000) Examination of the effect of the parameters of the two-circuit system of electroslag remelting on the dimensions and shape of the metal pool. *Advances in Special Electrometallurgy*, **4**, 3–7.
6. Protokovilov, I.V., Porokhonko, V.B. (2014) Methods to control metal solidification in ESR. *Sovrem. Elektrometall.*, **3**, 7–15.
7. Hou, Z., Dong, Y., Jiang, Z. et al. (2022) Effect of an external magnetic field on improved electroslag remelting cladding process. *Int. J. Miner. Metall. Mater.*, **29**, 1511–1521. DOI: <https://doi.org/10.1007/s12613-021-2277-3>
8. Soloviov, V.G., Kuskov, Yu.M. (2018) Influence of technological and electrical parameters of ESS in current-supplying mould. *The Paton Welding J.*, **6**, 20–27. DOI: <https://doi.org/10.15407/tpwj2018.06.03>
9. Matvienko, V.N., Mazur, V.A., Leshchinsky, L.K. (2015) Evaluation of shape and sizes of weld pool in surfacing using combined strip electrode. *The Paton Welding J.*, **9**, 28–31. DOI: <https://doi.org/10.15407/tpwj2015.09.04>
10. Tomilenko, S.V., Kuskov, Yu.M. (2000) Regulation and stabilization of base metal depth penetration in electroslag surfacing in current-supplying mould. *Svarochn. Proizvodstvo*, **9**, 32–35 [in Russian].
11. Sokolovskaya, L.A., Mamishev, V.A. (2009) Mathematical modeling of problems with phase transitions in metallurgy and foundry. *Protsessy Litya*, **2**, 24–29 [in Russian].
12. Liu, Fb., Zang, Xm., Jiang, Zh. et al. (2012) Comprehensive model for a slag bath in electroslag remelting process with a current-conductive mould. *Int. J. Miner. Metall. Mater.*, **19**, 303–311. DOI: <https://doi.org/10.1007/s12613-012-0555-9>
13. Makhnenko, O.V., Milenin, A.S., Kozlitina, S.S. et al. (2016) Optimizing technological process of electroslag melting of steel cylindrical ingots based on results of mathematical modeling. In: *Proc. of 8th Int. Conf. on Mathematical Modeling and Information Technologies in Welding and Related Processes, 19–23 September 2016, Odesa*, 96–101.
14. Zhiwen Hou, Yanwu Dong, Zhouhua Jiang et al. (2018) Simulation of compound rolls produced by electroslag remelting cladding method. *Metals*, **7**(8), 504. DOI: <https://doi.org/10.3390/met70504>
15. Kuskov, Yu.M., Soloviov, V.G., Lentugov, I.P., Zhdanov, V.A. (2018) Electroslag surfacing of layers of different thickness in stationary current-supplying mould. *The Paton Welding J.*, **10**, 33–36. DOI: <https://doi.org/10.15407/tpwg2018.10.06>
16. Ksendzyk, G.V. (1975) Current-supplying mould providing slag pool rotation. *Spets. Elektrometall.*, **27**, 32–40 [in Russian].
17. Gukhman, A.A. (1973) *Introduction to the theory of similarity*. 2nd Ed. Moscow, Vysshaya Shkola [in Russian].

ORCID

V.G. Solovyov: 0000-0002-1454-7520,
Yu.M. Kuskov: 0000-0002-8091-2274,
I.Yu. Romanova: 0000-0001-7154-1830

CONFLICT OF INTEREST

The Authors declare no conflict of interest

CORRESPONDING AUTHOR

V.G. Solovyov
E.O. Paton Electric Welding Institute of the NASU
11 Kazymyr Malevych Str., 03150, Kyiv, Ukraine.
E-mail: hsova@gmail.com

SUGGESTED CITATION

V.G. Solovyov, Yu.M. Kuskov, I.Yu. Romanova (2024) Optimization of the metal pool shape during electroslag surfacing in a stationary current-supplying mould for manufacture of bimetallic products. *The Paton Welding J.*, **5**, 28–36.

JOURNAL HOME PAGE

<https://patonpublishinghouse.com/eng/journals/tpwj>

Received: 21.02.2024

Received in revised form: 04.04.2024

Accepted: 10.06.2024